JOURNAL OF CATALYSIS 134, 434–444 (1992)

Structural and Surface Characterization of the Polycrystalline System $Cr_xO_y \cdot TiO_2$ Employed for Photoreduction of Dinitrogen and Photodegradation of Phenol

C. MARTIN,* I. MARTIN,* V. RIVES,*,[1] L. PALMISANO,† AND M. SCHIAVELLO†

*Dipartimento de Química Inorgánica, Universidad de Salamanca, Facultad de Farmacia, 37007-Salamanca, Spain; and †Dipartimento di Ingegneria Chimica dei Processi e dei Materiali, Universitá di Palermo, Facoltá di Ingegneria, Viale delle Scienze, 90128 Palermo, Italy

Received July 10, 1991; revised October 24, 1991

The polycrystalline system $Cr_xO_y \cdot TiO_2$, used as a catalyst for photoreactions, was studied by X-ray diffractometric method, visible-ultraviolet diffuse reflectance and infrared spectroscopic methods, surface area determination, and porosimetry to characterize its structural and surface features. Two series of catalysts were prepared by two different methods, namely by coprecipitation and by impregnation. The first series was tested as photocatalysts for the dinitrogen photoreduction in a gas–solid regime and for the phenol photodegradation in a liquid–solid regime. The results indicate that the interaction of chromium ions with OH groups modifies the surface properties of the supports and consequently influences the photocatalytic activity. The addition of Cr ions was found to accelerate the photoreduction reaction, while it is detrimental to the photodegradation of phenol.

INTRODUCTION

Heterogeneous photocatalysis by semiconductors is becoming a fast growing field of fundamental and applied research (*1–4*).

We have undertaken an investigation with the aim of studying bulk structural and surface properties of the polycrystalline system $Cr_xO_y \cdot TiO_2$, prepared by two different methods. X-ray diffractometry, BET surface area determination, reflectance and infrared spectroscopies, and porosimetry were used for catalyst characterization.

Samples of one preparation were also evaluated in two photocatalytic reactions, photoreduction of dinitrogen to ammonia in the presence of water vapor in a gas–solid regime, and photodegradation of phenol in aqueous dispersions. These data provided correlations between the bulk structural and surface properties of the catalysts and their photocatalytic properties. Papers on separate aspects of the whole investigation have been previously published (*5–8*).

[1] To whom correspondence should be addressed.

EXPERIMENTAL

Catalysts Preparation

One set of catalyst samples was prepared by impregnation (*7*) and the other by coprecipitation (*5*). The former catalysts are designated as TC-IM and the latter as TC-CP, followed by a number indicating the nominal Cr content (at.%).

Impregnation method. TC-IM samples (Cr/Ti = 1, 3, and 5 at.%) were obtained by impregnating TiO_2 (Degussa P25) heated overnight at 670 K to eliminate adsorbed organic residues with an aqueous solution (50 ml) containing desired amounts of CrO_3 (U.C.B., Belgium). After stirring for 60 min, the solvent was slowly evaporated at 330 K and the samples were dried overnight at 380 K. The yellow powder thus obtained was heated for 3 h at 770 K in the O_2 flow (30

0021-9517/92 $3.00

ml/min) and then was cooled to room temperature for 16 h.

Coprecipitation method. TC-CP samples (Cr/Ti = 0.2, 0.5, 1.0, 2.0, and 5.0 at.%) were obtained by reacting aqueous solutions of $TiCl_3$ (15 wt% Carlo Erba) containing the required quantity of Cr^{3+} ions (e.g., $Cr(NO_3)_3 \cdot 9H_2O$, Merck) with aqueous solutions of ammonia (25 wt%, Merck), which were added dropwise at room temperature with vigorous stirring (the reaction is exothermic). The solids were filtered and washed repeatedly to remove residual Cl-ions (tested as AgCl (s)). After standing for 24 h at room temperature, they were dried at 393 K for 24 h and finally fired in air for 24 h at 773 K.

Pure $TiO_2(TiO_2hp)$ was obtained following a procedure similar to the coprecipitation method described above for the Cr-doped samples.

X-Ray Diffractometry

X-ray diffraction patterns were recorded with a Rigaku Geiger-flex instrument using Ni filtered Cu$K\alpha$ (λ = 1.54050 A) radiation under standard conditions.

Diffuse Reflectance Spectroscopy

The spectra in the range 220–880 nm were recorded using a Shimadzu UV-240 spectrophotometer with a diffuse reflectance accessory. For reasons given below, MgO or TiO_2 was used as reference with a slit of 5 nm.

Infrared Spectroscopy

The infrared spectra were recorded with a Perkin–Elmer FT-spectrometer (Model 1730) coupled to a PE-3600 data station. A special Pyrex cell that allows recording of the spectra in vacuum or under a controlled atmosphere was used.

The procedure was performed as follows: the solid was compacted to a self-supported disc (1 cm diameter) weighing 50–60 mg and was calcined in air at 673 K for 2 h in the cell in order to eliminate any organic impurities adsorbed during the preparation. The sample was outgassed at 673 K for 2 h at a residual pressure of ca. 10^{-3} N m^{-2}, and, after cooling to room temperature, it was equilibrated with pyridine (pressure of 0.2 kN m^{-2}), and then outgassed for 30 min at temperatures increasing to 673 K.

Surface Area Determination and Porosity

Specific surface areas, SSA, of all of the catalysts were determined by N_2 adsorption at 77 K, using the dynamic BET method and a Micromeritics Flowsorb 2300 apparatus. Porosity assessment of the samples was carried out by nitrogen adsorption at 77 K in a conventional Pyrex high-vacuum apparatus (residual pressure ca. 10^{-4} N m^{-2}), equipped with a silicon oil diffusion pump and a Baratron MKS pressure transducer. Analysis of the data has been carried out with the assistance of a computer program developed by us (*9*).

Apparatuses and Procedures for the Photocatalytic Reactions

Dinitrogen photoreduction. The experiments lasted 3 h and were performed in a continuous apparatus with a fixed-bed photoreactor.

The lamp used was an Osram HWL (160 W). N_2 (99.95% purity) was fed at a constant flow rate of 0.4 cm^3 s^{-1} into the reactor together with H_2O vapor. The gas outflow from the reactor was passed through a 0.01 *N* HCl aq. solution to measure produced ammonia. The quantitative determination was performed by a standard colorimetric method (*10*).

In order to determine the amount of NH_3 adsorbed by the catalyst surface, the reactor was held for several hours at 573 K after the experiments, flushing it by helium. The ammonia evolved was trapped, and its amount measured by the same colorimetric method. Details on the apparatus and procedure can be found elsewhere (*5, 11*).

Phenol photodegradation. The experiment was performed using Pyrex glass flasks containing 50 ml of reacting mixture as photoreactors. All experiments were carried out by using concentrations equivalent to 1 g

liter^{-1} of powder and 90 × 10^{-3} g liter^{-1} of phenol at pH 3, 6, and 13. Stirred dispersions were irradiated by a 1500-W Xe lamp (Philips XOP 15-OF) inside a Solarbox 522 (CO. FO. ME. GRA., Milan) at 313 K. The photodegradation runs lasted 1.5 h. The samples were centrifuged immediately afterward, and the phenol concentration in the supernatant liquid was measured by a standard colorimetric method (*12*). Details on the apparatus and procedure can be found elsewhere (*5, 6, 13*).

RESULTS AND DISCUSSION

X-Ray Diffraction

TiO_2 (P25 Degussa) used to prepare TC-IM samples is a mixture of anatase and rutile, in the ratio of ca. 4 : 1 (*14*), judging by the intensities of the most intense diffraction peaks due to these two modifications of titania. This composition remains constant in all TC-IM samples studied. In the TiO_2hp and in TC-CP specimens, anatase is the major component, a small quantity of rutile detected only in sample TC-CP5.

Peaks due to a separate chromia phase were not detected in any samples. Apparently, a small amount of chromia existing in some of the samples is too low to be detected. In order to verify this conclusion, reference samples where prepared by mixing TiO_2 and Cr_2O_3 in a mortar in relative amounts identical to those existing in our samples. The X-ray diffraction patterns of these mixtures and of the samples containing the same relative amounts of chromium are included in Fig. 1. The most intense peak of Cr_2O_3 at d = 2.673 Å is absent in the sample with [Cr] = 1%, but it is readily identified in samples with [Cr] = 3 or 5%. These results indicate that our technique is sensitive enough to detect Cr_2O_3 in samples containing at least 3% Cr. Thus, the lack of detection of Cr_2O_3 diffraction peaks in the catalysts spectra should be due to good dispersion of the phases containing chromium within titania crystallites, probably because the calcination temperature in both sets of samples is too low to permit

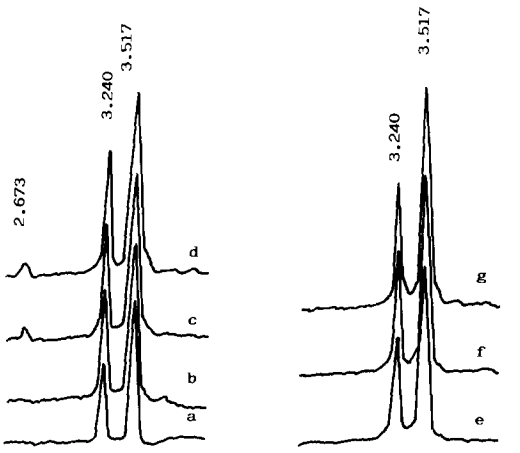

FIG. 1. X-ray diffraction patterns of (a) support TiO_2 P25; reference mixtures of Cr_2O_3 and TiO_2 containing (b) 1%, (c) 3%, (d) 5% Cr (atomic ratio); samples (e) TC-IM1, (f) TC-IM3, (g) TC-IM5.

diffusion of Cr^{3+} ions and formation of "bulk" Cr_2O_3. In any case, formation of a solid solution of chromia in titania could be the most approximate picture, at least in the few external layers of the titania crystallites.

Diffuse Reflectance Spectroscopy

The spectra of several samples are shown in Fig. 2. Due to strong absorption below

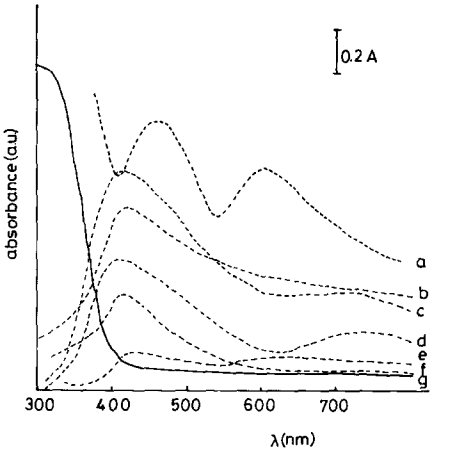

FIG. 2. V-UV spectra (diffuse reflectance) for samples: (a) Cr_2O_3; (b) TC-IM5; (c) TC-CP5; (d) TC-CP1; (e) mechanical mixture (1% Cr : Ti); (f) TC-IM1; (g) TiO_2 P25. Reference: spectra (a)–(f) support (TiO_2hp or TiO_2 P25); spectrum (g) MgO.

400 nm displayed by titania, the spectra have also been recorded using parent titania (Degussa P25 for samples TC-IM, and TiO_2hp for samples TC-CP) as references. Only the spectra for samples containing 1 and 5% Cr are shown. The other samples have spectra with bands in the same positions, but the intensities of which lie between those of the two samples shown in Fig. 2.

The intensities of the bands increase as the chromium content does. For samples TC-CP, two bands are recorded, one slightly above 700 nm and split, and the other one close to 400 nm. For samples TC-IM only a band at 400 nm is present (the position of which coincides with that for the TC-CP samples), but in this case a long tail is recorded in the high-wavelength side of the band.

The spectrum of bulk Cr_2O_3 shows two absorption bands at 600 and 455 nm that are ascribed to $A_{2g} \rightarrow T_{2g}$ and $A_{2g} \rightarrow T_{1g}$ *d-d* transitions. In chromia/titania samples, Borgarello *et al.* (*15*) attributed a band at 450 nm to a charge transfer transition from discrete energy levels of Cr^{3+} ions to the conduction band of titania. However, previous results reported by some of us (8) support a different assignment. A strong band at 410–420 nm was recorded in V-UV/DR spectra of oxide systems formed by oxides of transition metals (V^{5+}, Cr^{3+}, Mn^{2+}, Fe^{3+}, Ni^{2+}, Mo^{6+}) supported on titania and calcined under the same conditions as the samples studied here. Obviously, if such a band is due to a charge transfer from particular levels of the "guest" cation to the conduction band of titania, its position would change from one cation to another. In addition, the band would not be recorded for vanadia/titania (V^{5+}, d^0) and molybdena/titania (Mo^{6+}, d^0) systems, with no electron in the *d* orbitals of the guest cation. We have previously concluded (*8*) that such a band could be originated by peroxide-like species, stabilized on the surface of titania by the presence of these guest cations, as hydrogen peroxide-impregnated titania displays a strong band in this position of the spectrum. Formation of such peroxide species in nickel oxide supported on titania has been claimed elsewhere (*16*), and Ni^{2+}–O–O–Ti^{4+} bridging peroxide species were proposed.

Two sets of samples (TC-CP and TC-IM) differ with regard to their V-UV/DR spectra. As mentioned above, the second band can be distinguished at 700 nm for TC-CP samples, while, for samples TC-IM, a constant decrease in absorbance is observed as the wavelength increases. Thus, the band at 700 nm could correspond to the $A_{2g} \rightarrow T_{2g}$ transition observed at 600 nm for bulk chromia, while such a band is not clearly recorded for samples TC-IM. It may be stated that, in the TC-IM samples, Cr^{3+} ions (r = 0.755 Å) incorporated by impregnation in the titania lattice can occupy lattice positions, substituting Ti^{4+} ions (r = 0.745 Å), or can be located in interstitial sites, electrical balance being manitained by oxygen vacancies in the second coordination sphere (*17*). Because of this, the existence of Cr^{3+} cations in differently distorted environments (rutile, anatase, interstitial, substitutional sites) can lead to broadening of the Cr^{3+} *d-d* transition bands, thus extending their range above 400 nm. On the contrary, only the anatase phase exists in the TC-CP samples, and precipitation should lead to location of the Cr^{3+} in well-defined octahedral sites (more stabilized than the tetrahedral ones by crystal field splitting), leading to the expected *d-d* transition bands. However, the bands are recorded in different positions as a result of the formation of the anatase phase: the size of the $[MO_6]$ octahedron in chromia (corundum) and titania being different, the metal–ligand interactions are altered, thus leading to a shift of the $A_{2g} \rightarrow T_{2g}$ band toward higher wavelengths.

Our results are in agreement with those previously reported by Evans and coworkers (*18*) who have reported that chromium ions in rutile remain on the surface of the crystallites up to 773 K and that migration into the bulk to substitutional positions

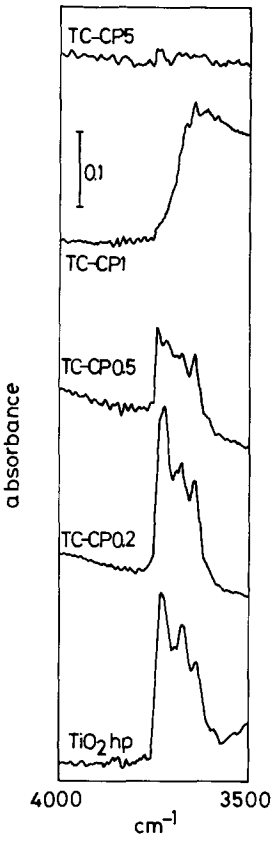

FIG. 3. FT–IR spectra of samples of series CP outgassed at room temperature for 2 h.

occurs only after calcination above this temperature, while with anatase this migration is hindered. On the contrary, when anhydrous precursor paste of titania is impregnated with an aqueous solution of Cr^{3+} ions prior to calcination (a situation similar to that existing in our TC-CP samples), and ESR signal attributed to chromium ions in substitutional sites of the anatase lattice is recorded.

Infrared Spectroscopy

The spectra for samples TiO_2hp and TC-CP in the 4000–3500 cm^{-1} range are reported in Fig. 3. TiO_2hp shows three absorption bands at 3726, 3673, and 3638 cm^{-1}, very close to those previously reported by Munuera *et al.* (*19*) for anatase. The spectrum of TC-CP0.2 sample is almost unchanged, the first band being slightly wider, with its main absorption at 3722 cm^{-1}, the other bands being recorded at 3673 and 3641 cm^{-1}. The situation, however, changes noticeably for TC-CP0.5 sample, the band separation becomes very poor, with hydroxyl stretching absorptions at 3737, 3715, 3675, and 3641 cm^{-1}. As the chromium content increases, changes in the spectra are more evident. So, the spectrum of TC-CP1 sample shows only very weak absorptions at 3666, 3643, 3612, and 3580 cm^{-1}, and, finally, no defined band is recorded for TC-CP5 sample. This behavior seems to be due to consumption of exposed anatase hydroxyl groups as the chromium content increases, which, in agreement with our previous results, indicates that chromium species are mainly located on the surface of titania crystallites. Support P25 and the samples prepared with it show a very similar behavior: the bands at 3720, 3672, and 3640 cm^{-1} are almost absent even in the sample containing 1% Cr.

Pyridine adsorption. The spectra recorded upon adsorption on supports and outgassing at increasing temperatures are included in Fig. 4, whereas those of the samples containing different amounts of chromium are given in Fig. 5. In the case of TiO_2hp, the bands corresponding to pyridine adsorbed on surface Lewis acid centers are at 1604, 1575, 1492, and 1445 cm^{-1}, the most intense bands at 1604 and 1445 cm^{-1} being the most characteristic of Lewis sites (vibration modes 8a and 19b of the pyridine ring, respectively). Upon outgassing at increasing temperatures, the band due to ν_{8a} mode shifts toward higher wavenumbers, from 1604 to 1613 cm^{-1}, but no splitting is observed, indicating that only one type of Lewis acid sites exists. This shift has been also reported by other authors (*20, 21*), but its origin remains unclear; Parfitt *et al.* (*20*) have correlated it to some sort of interaction between adsorbed pyridine and surface hydroxyl groups of the titania support.

In addition to this shift, the intensities of

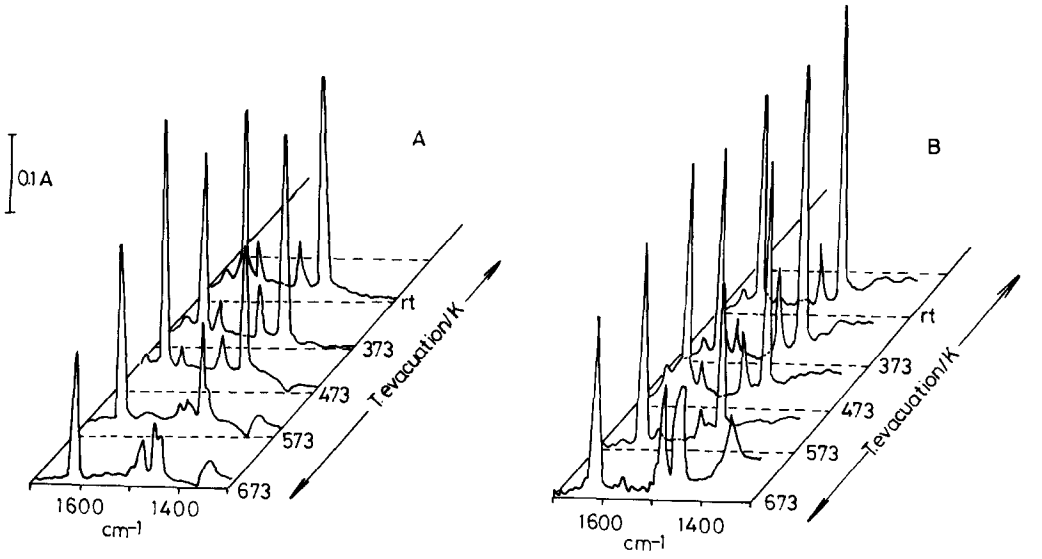

FIG. 4. FT–IR spectra showing adsorption of pyridine on supports (A) TiO_2 P25, and (B) TiO_2hp, upon outgassing at the indicated temperatures (for details, see text).

the bands decrease only very slightly as the outgassing temperature increases, thus indicating that the sites at which the pyridine molecules are adsorbed are strong acid centers, as the pyridine molecules are removed only after outgassing at fairly high temperatures. When outgassing is performed at 673 K, new bands appear at 1560, 1476, 1450, and 1440 cm^{-1}. These bands correspond to decomposition products of pyridine coordinated to surface sites. It should also be mentioned that the band at 1640 cm^{-1} could also be due to the ν_{8a} mode of pyridine adsorbed on Brønsted sites. However, in such a case another band should be at 1535 cm^{-1} (ν_{19b}), and this is not the case. So, we conclude

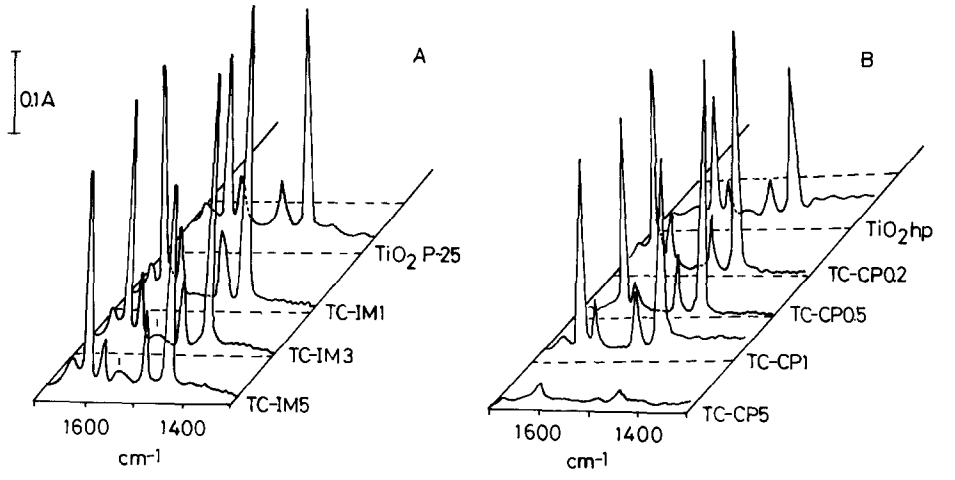

FIG. 5. FT–IR spectra after adsorption of pyridine and outgassing at room temperature for 30 min on samples belonging to series (A) TC-IM, and (B) TC-CP.

that only Lewis sites exist on the surface of the TiO_2hp support.

Busca *et al.* (*21*) have previously reported two types of Lewis sites on the surface of anatase, studied by infrared monitoring of adsorption of probe molecules, and in agreement with the model proposed by Munuera *et al.* (*19*) for the surface of anatase. According to the positions of the bands in the spectra (Fig. 4), the Lewis sites in our samples correspond to those named as "α-type" by Busca *et al.* (*21*) and are coordinatively unsaturated Ti^{4+} ions with a local symmetry C_{2v}, coordinated to four lattice oxide ions. The differences in the spectra of support P25 submitted to the same series of treatments are very small (Fig. 4A) when compared to the spectra of the TiO_2hp sample.

The samples containing chromium prepared on support TiO_2hp (Fig. 5B) again contain only Lewis sites, in agreement with very recent results reported by Chen and Chen (*22*). Development of Brønsted Cr–OH sites was not observed. In addition, a sharp decrease in the intensities of the bands is observed as the chromium content increases, thus indicating that the concentration of Lewis centers in sample TC-CP5 is negligible. However, as the chromium content increases, the outgassing temperature required to remove adsorbed pyridine is lower; that is, the strength of the Lewis sites decreases as the chromium content increases. Decomposition of pyridine is also observed at lower temperatures, and, for sample TC5, it takes place even upon outgassing at 473 K.

For samples belonging to series TC-IM, the IR bands are (Fig. 5A) at 1639, 1604, 1575, 1492, and 1448 cm^{-1} (sample TC-IM1), thus indicating adsorption of pyridine on Lewis acid sites. For samples TC-IM3 and TC-IM5 the bands originated by Lewis acid sites are at 1640, 1606, 1575, 1491, and 1445 cm^{-1}, but, in addition, a weak band is recorded at 1542 cm^{-1}. It has been ascribed to the ν_{19b} mode of pyridinium ion. This result represents a difference with regard to samples belonging to series TC-CP, where no indication of the existence of Brønsted sites was found. This type of site is, however, in samples containing chromium, but prepared on titania from Degussa, although only a small proportion of such sites seems to exist. An additional difference between both series of samples is that in those prepared on support P25 the intensities of the bands decrease steadily as the chromium content increases, while in those prepared on support TiO_2hp such a decrease is very rapid.

With regard to the spectral changes for the samples with different chromium content, the behavior observed is similar to that reported for samples belonging to TC-CP series: as the chromium content increases, pyridine decomposition is observed at lower temperatures; so, decomposition takes place at 573 K for sample TC-IM1, but it is already evident upon outgassing samples TC-IM3 and TC-IM5 at 473 K.

The areas of the band originated by the ν_{19b} mode of pyridine can be taken as indicative of the amount of Lewis sites in the samples. These areas (calculated with a subroutine provided in the Data Station software) have been plotted in Fig. 6 vs the chromium content in the samples. For samples belonging to the TC-CP series the band area slightly increases for very low chromium content and then decreases as the Cr content increases. For samples corresponding to TC-IM series such a decrease is also evident, but less pronounced. The overall decrease of surface acid sites should be partially compensated, at least in samples TC-IM3 and TC-IM5, with development of Brønsted sites, as shown above.

Surface Area and Porosity

Values for specific surface area (SSA) of the samples have been summarized in Table 1. TC-IM samples show a slight decrease in the SSA values as the chromium content increases, while an *increase* in SSA is observed for TC-CP samples. Nitrogen adsorption and the pore size distribution was

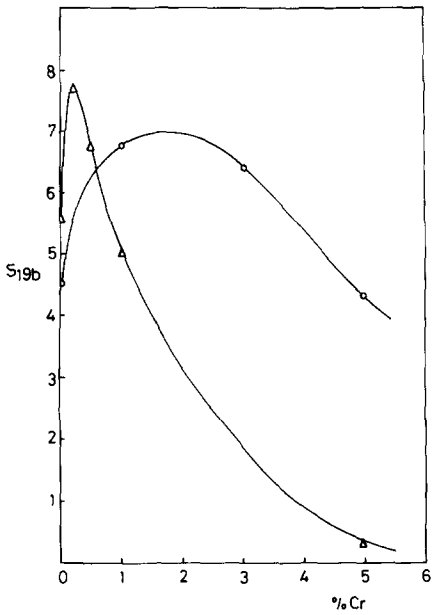

FIG. 6. Change in the area of the ν_{19b} band of adsorbed pyridine on Lewis sites vs the Cr content. (△): series TC-CP; (○): series TC-IM.

studied for all samples. No significant difference is observed between the textural properties of the support and those of the chromium-containing TC-IM samples, in contrast to the TC-CP specimens. Moreover, the textural features of the P25 support are similar to those of TiO_2hp sample.

TABLE 1

Specific Surface Area (SSA) Values of the Samples Studied ($m^2\ g^{-1}$)

Sample	SSA
TiO_2hp (support)	51
TC-CP0.2	73
TC-CP0.5	75
TC-CP1	60
TC-CP2	44
TC-CP5	58
TiO_2 P25 (support)	49
TC-IM1	46
TC-IM3	46
TC-IM5	44

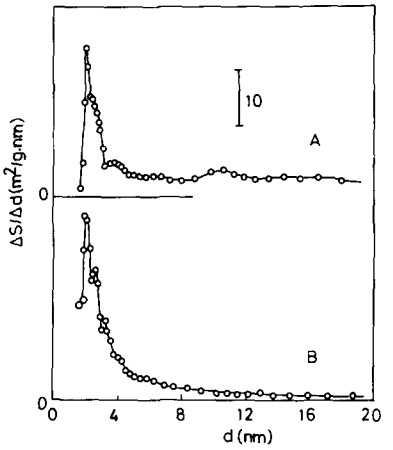

FIG. 7. Pore size distribution curves for samples (A) TC-CP1, and (B) TiO_2hp.

All isotherms belong to type II according to the IUPAC's classification (*23*). The adsorption is reversible for the TiO_2hp sample and, as the percentage of chromium increases, a hystheresis loop is observed for high relative pressures. Its shape has been associated with a development of pores in aggregates, thus explaining the observed increase in the SSA. As a consequence, there is a contribution to the surface area from the large pores thus formed, as shown by the pore size distribution curves shown in Fig. 7. The main contribution to the surface area for the TiO_2hp support comes from pores with a diameter of 2–3 nm. In the case of the TC-CP1 sample (and, in general, all TC-CP samples) a contribution by larger pores is also observed. Finally, the *t* plots in Fig. 8 for support TiO_2hp and sample TC-CP1 also show some differences: the plot for the support is linear, while that for the sample containing chromium deviates upward for large values of the depth of the adsorbed nitrogen layer, indicating an increased uptake of nitrogen due to condensation in larger pores (*24*).

Summary of the Photocatalytic Reaction Studies

The TC-CP specimens as well as the pure compounds, TiO_2 and Cr_2O_3, were tested.

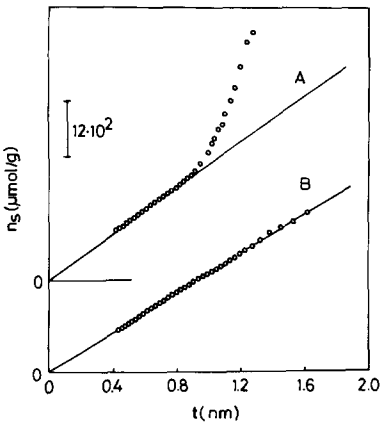

FIG. 8. *t*-plots for samples (A) TC-CP1, and (B) TiO_2hp.

For the photoreduction of dinitrogen, the reactivity of pure compounds was found not detectable, while that of the TC-CP specimens varied from 8.3 to 96.4 $\mu g\ h^{-1}\ m^{-2}$, the most photoreactive being TC-CP 0.5. These values refer to the total ammonia produced (released in the gas phase during the experiments and desorbed from the surface after the experiments). This latter was found to decrease as the Cr addition increased.

For the phenol photodegradation experiments it was found that TiO_2hp is photoactive at any pH. It was also observed that pure Cr_2O_3 is not active while the TC-CP specimens have photoactivity lower than or similar to that of TiO_2 (*5*). Thus, addition of Cr ions to titania has a beneficial effect on the photoreduction of dinitrogen and is detrimental to the photodegradation of phenol. The contrasting behavior of the additions of Cr^{3+} ions (positive for the dinitrogen photoreduction, indifferent or detrimental to the phenol photodegradation) was explained elsewhere in detail (*5*). In the present paper we present only a general picture.

Dinitrogen photoreduction. The addition of Cr^{3+} ions in the lattice of titania (the solid solution specimens) is beneficial for at least two reasons: (i) it enhances the separation of the photogenerated pairs since it builds up a space charge region (*25*), while for the heavily doped specimens this is not possible; and (ii) it improves the capability by the solid to adsorb N_2 molecules as the concentration of Ti^{3+} species increases in the presence of the dopant; it has been also reported (*26*) that titania specimens containing Cr^{3+} are able to activate N_2 at room temperature.

Phenol photodegradation. In this case, pure TiO_2 (anatase) is suitable, both from the thermodynamic and kinetics points of view (*27*), to efficiently perform the reaction, and the addition of chromium ions is only ineffective or detrimental, depending on its content and on the initial pH of the dispersion (*5*). Indeed, as reported above, the acid–base reaction between Cr^{3+} and hydroxyl groups leads to a decrease in the surface concentration of the latter. It is well known (*28*) that the essential role of these hydroxyl groups in the photodegradation of pollutants in aqueous dispersions as the oxidative attack to the substrates mainly occurs by photoproduced $OH^{\cdot}$ radicals. Therefore, the presence of chromium is ineffective for low levels of doping, when the surface properties, and in particular the surface hydroxylation, of pure titania are slightly modified, but it is detrimental for high level of doping, when the presence of surface OH groups becomes negligible and insufficient for the occurrence of the photoreaction.

CONCLUSIONS

The examination of the results suggests several considerations about the nature of the interaction between Cr ions and the titania lattice and about the photocatalytic behavior for the two photoreactions.

(1) The interaction between Cr ions and the titania lattice is quite indifferent to the preparation methods, which have the same firing temperature and differ in the starting materials and in the procedures.

(2) Chromium ions are well dispersed in the top layers of titania (mainly anatase) surface. The fact that chromium oxides are not detectable by the X-ray method and that the firing temperature (773 K) was rather low suggests the formation of a "surface" solid

solution and/or the formation of very small crystals of chromium oxides well dispersed on the surface of the anatase.

(3) Both supports (TiO_2 P25 and TiO_2hp) have a variety of OH groups of different nature and different acid–base strength on the surface. Chromium ions interact with the OH groups decreasing their content as the concentration of Cr ions increases. It is in the extent and the nature of this interaction that the samples, prepared by the two different methods, manifest the marginal differences. If one considers the interaction between chromium ions and the OH groups on the surface as an acid–base interaction, it is understandable why the TC samples prepared by the two different methods behave differently. These differences are evident in the residual acidity, since a small amount of Brønsted acidity is detectable on the TC-IM specimens, while the Brønsted acidity is not present in the TC-CP specimens. In the behavior of the specific surface areas a small difference is also manifest, probably due to a different development of the various sizes of the pores: in the TC-CP the macropores are predominant (*5*).

(4) As for the photocatalytic features of both photoreactions, the major role of the OH groups has been stressed in previous papers (*5, 6, 11, 13*) and the results of the present study add information to the understanding of some details. The FT–IR results confirm the presence of a variety of OH groups on the surface of both series of specimens studied. These groups can (i) trap the holes of the photogenerated pairs, influencing the recombination–separation rate, (ii) enter in the reaction mechanism, (iii) favor the formation of peroxide groups, which have been invoked to explain features of the photoreactivity for other specimens ($Fe_xO_y \cdot TiO_2$) previously studied (*11*), and (iv) influence the adsorption and desorption of reagents and products.

Finally, it is worth stressing the different role played by the different gas–solid and liquid–solid interfaces. Indeed, the space-charge layer developed in the liquid–solid interface is sufficient, as indicated by the photoreactivity results, to hasten the pair separation and consequently the occurrence of the phenol degradation on pure titania (anatase). On the contrary, the presence of chromium is essential in a gas–solid regime for dinitrogen photoreduction.

ACKNOWLEDGMENTS

L.P. and M.S thank Ministero dell'Università e della Ricerca Scientifica e Tecnologica (Roma) for finantial support. I.M. acknowledges a grant from DGICYT (Spain).

REFERENCES

1. Schiavello, M., Ed., "Photoelectrochemistry, Photocatalysis and Photoreactors: Fundamentals and Developments." Reidel, Dordrecht, 1985.
2. Pelizzetti, E., and Serpone N., Eds., "Homogeneous and Heterogeneous Photocatalysis." Reidel, Dordrecht, 1985.
3. Schiavello, M., Ed., "Photocatalysis and Environment: Trends and Applications." Kluwer, Dordrecht, 1988.
4. Pelizzetti, E., and Serpone, N., Eds., "Photocatalysis: Fundamentals and Applications." Wiley, New York, 1989.
5. Palmisano, L., Augugliaro, V., Sclafani, A., and Schiavello, M., *J. Phys. Chem.* **92,** 6710 (1988).
6. Augugliaro, V., Palmisano, L., Sclafani, A., Minero, C., and Pelizzetti, E., *Toxicol. Environ. Chem.* **16,** 89 (1988).
7. Criado, J. J., Macías, B., and Rives, V., *React. Kinet. Catal. Lett.* **27,** 313 (1985).
8. del Arco, M., Holgado, M. J., Martin, C., and Rives, V., *Spectrosc. Lett.* **20,** 201 (1987).
9. Rives, V., SAPO programme, version 4.5. University of Salamanca, 1991.
10. Henry, J. M., Cannon, M. M., and Winkelman, T. A., "Clinical Chemistry: Principles and Techniques." Harper and Row, New York, 1978.
11. Soria, J., Conesa, J. C., Augugliaro, V., Palmisano, L., Schiavello, M., and Sclafani, A., *J. Phys. Chem.* **95,** 274 (1991).
12. Taras, H. J., Greenberg, A. E., Hoak, R. D., and Rand M. C., "Standard Methods for the Examination of Water and Waste-Water," 13th ed. American Public Health Association, Washington DC, 1971.
13. Augugliaro, V., Davi, E., Palmisano, L., Schiavello, M., and Sclafani, A., *Appl. Catal.* **65,** 101 (1990).
14. Bickley, R. I., Gonzalez-Carreño, T., Lees, J., Palmisano, L, and Tilley, R. J. D., *J. Solid State Chem.* **92,** 178 (1991).
15. Borgarello, E., Kiwi, J., Graetzel, M., Pelizzetti,

E., and Visca, M., *J. Am. Chem. Soc.* **104,** 2996 (1982).
16. Espinos, J. P., Gonzalez-Elipe, A. R., Munuera, G., Garcia, J., Conesa, J. C., and Burattini, E., *Phys. B* **158,** 174 (1989).
17. Sochava, L. S., Reshina, I. I., and Mirlin, D. N., *Fiz. Tverd. Tela* **12,** 1214 (1970); *Sov. Phys.-Solid State* **12,** 946 (1970).
18. Amorelli, A., Evans, J. C., Rowlands, C. C., and Egerton, T. A., *J. Chem. Soc. Faraday Trans. 1* **83,** 3541 (1987).
19. Munuera, G., Moreno, F., and González, F., *in* "Proceedings, 7th Int. Symp. on Reactivity of Solids," p. 681. Chapman & Hall, London, 1973.
20. Parfitt, G. D., Ramsbotham, J., and Rochester, C. H., *J. Chem. Soc. Faraday Trans. 1*, 1500 (1971).
21. Busca, G., Saussey, H., Saur, D., Lavalley, J. C., and Lorenzelli, V., *Appl. Catal.* **14,** 245 (1985).
22. Chen, S., and Chen, S. Y., *J. Catal.* **122,** 1 (1990).
23. Sing, K. S. W., Everett, D. H., Haul, R. A. W., Moscou, L., Pierotti, R. A., Rouquerol, J., and Sieminiewska, T., *Pure Appl. Chem.* **57,** 603 (1985).
24. Lowell, S., and Shields, J. E., "Power Surface Area and Porosity." Chapman & Hall, London, 1984.
25. Maruska, H. P., and Ghosh, A. K., *Solar Energy Mater.* **1,** 237 (1979).
26. Burch, R., and Flambard, A. R., *J. Chem. Soc., Chem. Commun.*, 965 (1981).
27. Sclafani, A., Palmisano, L., and Davi, E., *New J. Chem.* **14,** 265 (1990).
28. Turchi, C. S., and Ollis, D. F., *J. Catal.* **122,** 178 (1990).